Blue-Enhanced Supercontinuum Generation in a Graded-Index Fluorine-Doped Multimode Fiber

Z. Sanjabi Eznaveh [1*], M.A. Eftekhar[1], J.E. Antonio Lopez[1], M. Kolesik[2], H. Lopez Aviles[1], F. W. Wise[3], D. N. Christodoulides[1], and R. Amezcua Correa[1]

[1]*CREOL, The College of Optics and Photonics, University of Central Florida, Orlando, Florida 32816, USA*
[2]*College of Optical Sciences, University of Arizona, Tucson, AZ 85721, USA.*
[3]*School of Applied and Engineering Physics, Cornell University, Ithaca, New York 14853, USA.*
**Corresponding author: zahoora@knights.ucf.edu*

Abstract: We demonstrate blue-enhanced white-light supercontinuum generation in a fluorine-doped parabolic-index multimode fiber. The spectrum expands from 450–2,400nm with excellent spectral flatness and a beam quality factor of M^2~1.7 at 1064nm.

OCIS codes: (190.4370) Nonlinear optics, fibers; (190.4410) Nonlinear optics, parametric processes; (190.4380) Nonlinear optics, four-wave mixing; (060.0060) Fiber optics and optical communications

1. Introduction

Supercontinuum (SC) generation in optical fibers has found extensive applications in spectroscopy, optical metrology, and biomedicine [1]. Thus far, photonic crystal fibers (PCFs) with a flexible dispersion characteristics and high nonlinearity resulting from their small mode area, have been particularly successful in generating efficient SC that can span a few optical octaves [1–3]. To enhance the visible range of the SC spectrum, tapered PCFs, and PCFs with engineered dispersion characteristics have been employed [4,5]. Nevertheless, the maximum spectral power density that can be delivered by PCFs is limited due to their small core size. On the other hand, multimode fibers (MMFs) have recently attracted considerable attention for next-generation telecommunications systems [6], nonlinear dynamics studies [7,8] and high power fiber lasers [9]. In highly multimode graded index fibers, periodic spatial beam refocusing events can lead to a geometric parametric instability (GPI) in both anomalous and normal dispersive regimes. Accordingly, a series of intense frequency components in the visible and near-infrared (NIR) spectral region can be generated which eventually evolve into SC [7,10,11]. However, previous SC experiments based in Ge-doped GI-MMF required long fiber lengths (>25 m) in order to extend the spectra into the visible.

Here, we present the generation of flat, white-light SC generation in a 10 m long, in-house fabricated fluorine-doped parabolic-index MMF pumped at the normal dispersion regime with a peak power of up to 185 kW. The fluorine-doped fiber was intentionally used in order to further shift the short-wavelength edge of the spectrum towards the blue region using relatively short fibers [12]. The GPI-induced frequency generation was found to cover a broad spectral range (450 nm to 2400 nm). The spectral evolution of the continuum was recorded as a function of pump power. In addition, near-field images of the output mode profiles appeared to be Gaussian-like and speckle-free, showing a beam quality factor (M^2) of ~1.7 at 1064 nm. Our experimental observations are in very good agreement with numerical simulations. To the best of our knowledge, this is the first time that control over the material composition of GI-MMF is exploited for tailoring nonlinear propagation dynamics in such complex waveguides.

2. Experiments and simulations

The single mode output of an amplified Q-switched microchip laser, delivering pulses of duration 400 ps at 1064 nm with an energy of 95 μJ and 500 Hz repetition rate, was coupled into the MMF. A half-wave plate and a polarizing beam splitter cube were used in order to control the power, and polarization orientation of the input beam. A large number of transverse spatial modes were excited by focusing the laser beam to the front facet of the fiber and the output light was collected by a multimode patch cord and analyzed using two optical spectrum analyzers (OSAs) covering the spectral range from 350 nm to 2400 nm (ANDO AQ 6315E and Yokogawa AQ6375). The beam profiles at the output of the fiber was recorded using suitable infrared and visible cameras. The fiber used in our experiments was an in-house fabricated fluorine-doped GI-MMF with a core diameter of 50 μm and a maximum refractive index depression of ~-18×10^{-3} with respect to pure silica.

Figure 1 exhibits the generated SC spectrum in a 10 m long fluorine-doped fiber pumped at a peak power of ~185 kW. One can clearly observe that the spectral broadening takes place on both sides of the pump, generating a rather flat SC, from 450 nm to 2400 nm with intensity variations of less than 5 dB in the visible and less than 7 dB

in the NIR range of the spectrum. As we will see later, the visible spectrum generation mainly arises from multipath four-wave-mixing (FWM) interactions and periodic spatial beam refocusing taking place in the parabolic-index waveguides.

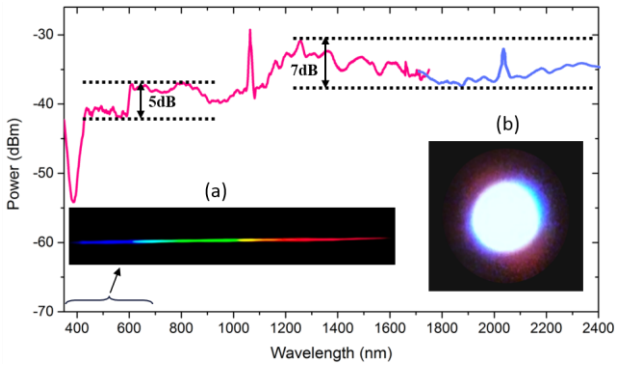

Fig. 1. SC spectra obtained in a 10 m long fluorine-doped GI-MMF using 185 kW peak pump power at 1064 nm. Red and blue spectra were recorded using two different OSAs. Inset: Grating-dispersed fiber output (a) and far-field pattern of the white light output beam (b).

A typical image of the relatively flat visible spectrum produced in a 10 m long fiber at ~185 kW is shown in the inset of Fig. 1(a), after being dispersed by a diffraction grating. This image shows a remarkably uniform spectrum that extends from deep red to blue/violet. In addition, a far field image of the output beam at the highest pump power is shown in inset of Fig. 1(b), demonstrating an essentially white light intensity distribution. Subsequently, the near-field spatial mode distributions were recorded at various wavelengths using 10 nm bandpass filters and appropriate imaging cameras (see Fig. 2). As Fig. 2 shows, at the highest pump power level (185 kW), the spatial mode profiles are Gaussian-like and no evidences of spackled patterns can be observed.

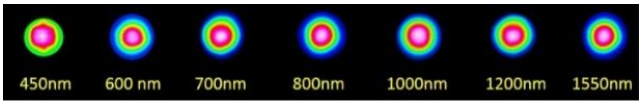

Fig. 2. Near-field pattern of the beam profiles at the output of a 10 m fluorine-doped MMF at 185 kW pump power, using 10 nm bandpass filters.

We have studied the spectral broadening dynamics and SC generation in our fluorine-doped GI-MMF as a function of the input pump power. Figure 3 shows SC spectra recorded at different pump power levels (28-185 kW) in a 5 m long fiber. It should be noted that here a short piece of fiber was used to enhance the visibility of distinct spectral features. As Fig. 3(a) shows, at low input pump power (~28 kW), two bands arising from Raman interactions and self-phase modulation can be clearly observed along with the pump signal. At 85 kW, additional discrete frequency peaks appear in the spectrum (Fig. 3(b)). As the pump power was further increased to 125 kW, the spectrum starts to exhibit a continuous broadening on both sides of the pump wavelength. At even higher pump powers (~185 kW), extremely wide spectral broadening of the input pulse occurs, extending from ~0.2 PHz (1500 nm) to more than 0.8 PHz (380 nm).

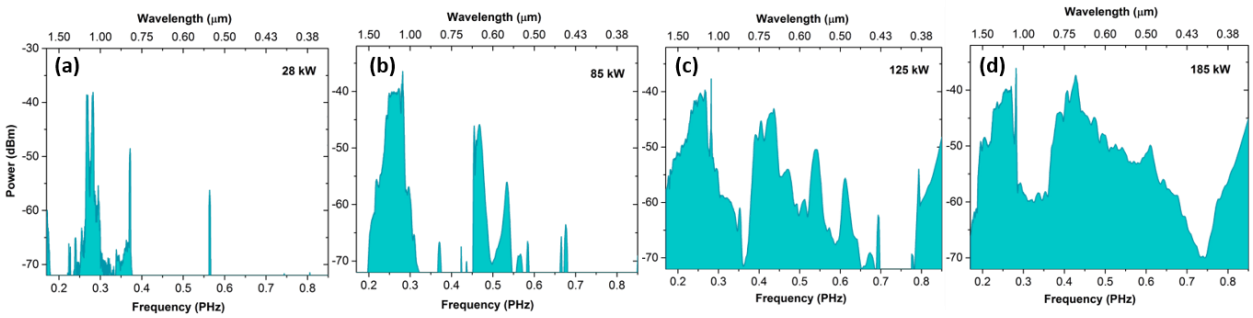

Fig. 3. SC evolution as a function of pump power in a 5m fluorine-doped MMF. The input power is (a) 28 kW, (b) 85 kW, (c) 125 kW, and (d) 185 kW.

Furthermore, numerical simulations were performed based on a general unidirectional pulse propagation equation (gUPPE) method in which the spatiotemporal evolution of the total electric field in the presence of linear (dispersion, guiding) and nonlinear effects (self-phase modulation, FWM, third harmonic generation, shock and Raman effects) is computed for hundreds or thousands of modes, simultaneously [13]. In our simulations, the time window, the size of the spatial window and an adaptive integration step size were 6 ps, 50 µm × 50 µm and 1-2 µm, respectively. To shorten the computation time, the propagation distance was set to 35 cm and the pulse width was taken to be 400 fs, with a beam waist of 27 µm.

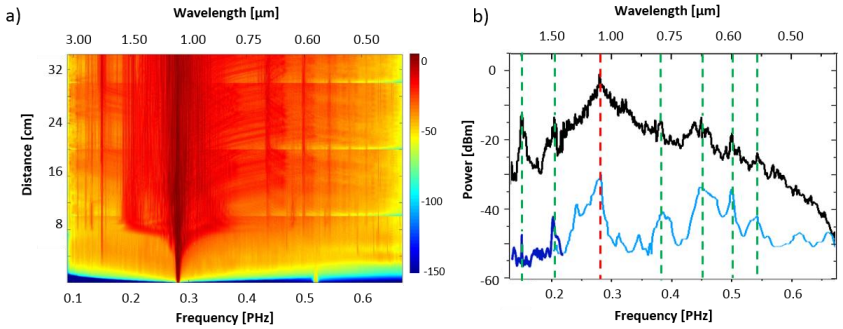

Fig. 4. (a) Spectral evolution upon propagation in a ~35 cm fluorine-doped GI-MMF. (b) Simulated (black curve) and measured (blue curve) spectra in the MMF. The red dotted line represents the position of the pump at 1064 nm while the green lines indicate the position of the expected GPI induced sidebands. The light/dark blue plots were recorded using two OSAs in order to cover the entire spectral regime of 350-2400 nm.

Figure 4(a) illustrates the spectral evolution of SC as a function of propagation distance in the fluorine-doped GI-MMF. In this figure, the spectral broadening due to self-phase modulation can be clearly observed during the early stages of propagation. After about 5 cm of propagation, the first GPI induced NIR line at ~2 µm appears. Subsequently, after ~10 cm, a series of visible and NIR sidebands emerge with the first ones located at 560 nm, 600 nm and 700 nm. More spectral features eventually develop as a result of Raman and FWM, resulting in a broad SC light extending from below 0.1 PHz to above 0.65 PHz. Figure 4(b) compares the experimentally observed frequency side-bands with numerical simulations. The spectra were measured using two OSAs covering the entire spectral range of 350-2400 nm. In this figure, the black and blue curves illustrate the simulated and measured spectra, respectively. As this figure indicates, there is excellent agreement between the experimental observations and numerical simulations.

3. Conclusion

In summary, we demonstrated the generation of a flat, blue-enhanced, white-light SC in a 10 m long fluorine-doped GI-MMF using 400 ps pump pulses at 1064 nm. The spectral broadening was shown to arise mainly from the induced GPI effects in this parabolic fiber and the combined action of SRS and FWM, in good agreement with numerical simulations. Our experiments show that tailoring the material composition of GI-MMF is an effective way of controlling the propagation dynamics in these fibers and opens up new opportunities for designing high power fiber sources.

Funding. This work was supported by ONR (MURI N00014-13-1-0649), HEL-JTO and ARO (W911NF- 12-1-0450), AFOSR FA9550-15- 10041.

4. References

[1] J. M. Dudley, et al., "Supercontinuum generation in photonic crystal fiber," Rev. Mod. Phys. **78**, 1135–1184 (2006).
[2] J. K. Ranka, et al., "Visible continuum generation in air–silica microstructure optical fibers with anomalous dispersion at 800 nm," Opt. Lett. **25**, 25–27 (2000).
[3] W. J. Wadsworth, et al., "Supercontinuum generation in photonic crystal fibers and optical fiber tapers: a novel light source," JOSA B **19**, 2148–2155 (2002).
[4] C. Xiong, et al., "Enhanced visible continuum generation from a microchip 1064nm laser," Opt. Express **14**, 6188–6193 (2006).
[5] R. R. Gattass, et al., "Supercontinuum generation in submicrometer diameter silica fibers," Opt. Express **14**, 9408–9414 (2006).
[6] D. J. Richardson, et al., "Space-division multiplexing in optical fibres," Nat. Photonics **7**, 354–362 (2013).
[7] L. G. Wright, et al., "Controllable spatiotemporal nonlinear effects in multimode fibres," Nat. Photonics **9**, 306–310 (2015).
[8] Z. S. Eznaveh, et al., "Tailoring frequency generation in uniform and concatenated multimode fibers," Opt. Lett. **42**, 1015–1018 (2017).
[9] D. J. Richardson, et al., "High power fiber lasers: current status and future perspectives [Invited]," JOSA B **27**, B63–B92 (2010).
[10] K. Krupa, et al., "Observation of geometric parametric instability induced by the periodic spatial self-imaging of multimode waves," Phys. Rev. Lett. **116**, (2016).
[11] G. Lopez-Galmiche, et al., "Visible supercontinuum generation in a graded index multimode fiber pumped at 1064 nm," Opt. Lett. **41**, 2553–2556 (2016).
[12] M. Oto, et al., "Optical fiber for deep ultraviolet light," IEEE Photonics Technol. Lett. **13**, 978–980 (2001).
[13] J. Andreasen, et al., "Nonlinear propagation of light in structured media: Generalized unidirectional pulse propagation equations," Phys. Rev. E **86**, 036706 (2012).